International Journal of Fluid Power 6 (2005) No. 2 pp. 19-36

AN INVESTIGATION OF SWASH PLATE CONTROL CONCEPTS FOR DISPLACEMENT CONTROLLED ACTUATORS

Joerg Grabbel[1)] and Monika Ivantysynova[2)]

[1)]*B+V Industrietechnik GmbH, ThyssenKrupp Technology AG, Hermann-Blohm-Strasse 5, 20457 Hamburg, Germany*
GrabbelJ@tkt-bvi.thyssenkrupp.com
[2)]*Purdue University, Department of Agricultural and Biological Engineering, 225 S. University Street, West Lafayette, IN 47907, USA*
Mivantys@purdue.edu

Abstract

Displacement controlled actuators offer a very promising alternative and energy saving solution for many applications in mobile machines, mobile robots and other applications. Here, the achievable system dynamics and thus the dynamics of the control element, the variable displacement pump, is often of great concern. It will be shown in this paper that electro-hydraulic pump control allows sufficiently high dynamics for this class of heavy duty actuators, which can in fact compete with conventional valve controlled systems.

Keywords: displacement controlled actuator, swash plate control, Ackermann parameter space method, rotary actuator

1 Introduction

Hydraulic drive technology offers a variety of different system solutions for a wide range of applications. In off road vehicles and mobile machines, where the hydraulic system is typically powered from the Diesel engine directly, today mostly valve controlled systems are installed. Since in these machines usually several hydraulic actuators have to work simultaneously, the use of valve controlled systems seems to be a straight-forward solution. One or two pressure compensated or load-sensing controlled pumps are usually installed to supply the individual valve controlled actuators. Although this design appears simple it is not necessarily cost effective, neither with respect to component expenditure nor to operating costs. Basic disadvantages are high installations costs for valve blocks, fittings and the large control valves themselves as well as comparatively low energetic efficiency due to the throttle losses since using control valves as final actuator control elements is effectively a control system using variable resistances. Furthermore, in case of closed loop control the load sensing solution has additional side effects, such as complex multi-variable controller design (as it a combined pressure and axes control) with a significant tendency to pressure oscillations, widely observed due to rapidly changing operating conditions. Additionally, load sensing systems have higher component and installation costs compared to a constant pressure system. However, it must be pointed out, that automation of mobile machinery, such as user-friendly operation of the tool-head in Cartesian coordinates or other computer assisted functions require closed loop control of all actuators of the working hydraulics of these machines.

In stationary equipment, like e.g. machine tools, where all actuators work in closed loop control, but also in mobile applications, where a sufficiently large electric power supply is available, like ships or aircrafts, different solutions, based on pump control (flow induced systems) were developed and successfully implemented. Pump controlled design basically offers two different solutions.

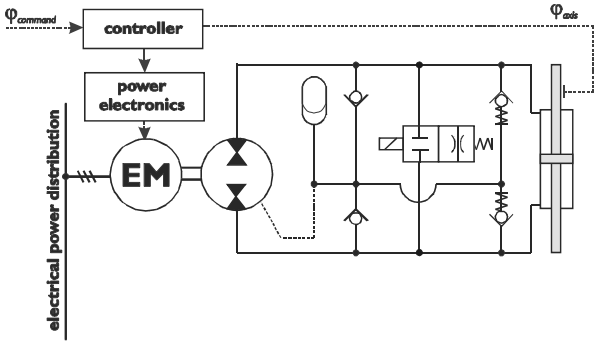

Fig. 1: *Displacement control – variable shaft velocity*

This manuscript was received on 24 May 2004 and was accepted after revision for publication on 6 June 2005

On the one hand there is a fixed displacement pump powered by an electrical motor at different speeds. A typical example related to an aircraft actuator solution is shown in Fig. 1. Although a double rod cylinder is the common actuator here, also a single rod cylinder or vane motor actuators are possible.

The speed control of the motor defines the delivered flow – thus, the speed control of the electrical motor is the control element of the system. Its dynamics, basically dominated by the inertia of the electric motor, define the achievable dynamics of the control element.

A second option is given by the use of a variable displacement pump driven by an engine or electric motor at constant speed. The delivered flow is defined by the adjustable displacement volume of the pump, making the pump control system the final controlling element of the actuator (see Fig. 2). Here the achievable dynamics are dominated by the pump control system, where the inertia of the moving parts is significantly lower compared to a fixed displacement pump - variable speed actuator solution.

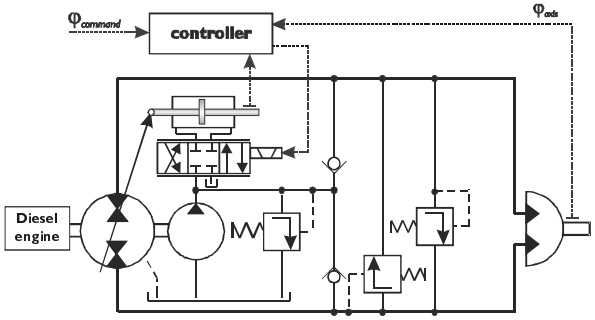

Fig. 2: *Displacement controlled rotary actuator*

The major advantage of a displacement pump controlled actuator compared to valve controlled solutions is a significantly higher efficiency, since there are no throttle losses within the main power lines of the actuators. Further, the characteristics are almost pressure independent and thus linear in a very wide operating range, where a valve controlled system shows a significant drop in valve flow with increased system load and thus a highly non-linear behaviour depending on the load conditions. Further, pump controlled systems offer the ability to recover energy in case of aiding loads by simply running the pump in motoring mode and driving other systems, which are mechanically connected to the machine drive line, e.g. steering system, hydrostatic transmission or even other actuators working simultaneously.

Although many advantages count in favour for pump controlled systems, a major and often heard prejudice, when it comes to pump control and achievable system dynamics, is that pump controlled systems are assumed to be unacceptably slow compared to valve controlled systems - identical load conditions assumed for both. This prejudice may somehow be explained by experience with the majority of pumps currently available on the market. The response time of these pumps is very often kept slow by using additional orifices to allow the use of these pumps in human controlled systems, e.g. hydrostatic transmissions. Usually pump control uses simple proportional control, often combined with mechanical feedback.

As already mentioned the inertia of the moved parts of a variable pump is significantly lower than the inertia of a fixed displacement/variable speed drive. Consequently, it is expected that this approach to pump control is likely to offer a much faster system, i.e. a higher system bandwidth. However, to determine the achievable dynamics in detail, the control system of a typical servo pump – a variable displacement overcenter pump with an electro-hydraulic pump control system has to be studied thoroughly. Here, a swash plate axial piston pump appears to be the most promising solution, since its design allows fast response times. Although radial piston pumps may also be suitable.

2 State of the Art

Hahmann (1973) and Berbuer (1988) investigated the dynamics of servo pump control systems considering self adjusting forces, based on the use of nonlinear models. Their approaches were validated experimentally by pressure measurements in both chambers of the pump control cylinder. These investigations were basically undertaken for developing control concepts for secondary controlled hydraulic motors. Also other authors proposed linearised models of first or second order for the pump control system (Sprockhoff 1979, Roth 1983), were non-linear effects like flow and stroke limitation were neglected. Others, like Ziegler (1990) and Backé (1993), suggested non-linear models of higher order to include non-linear effects. Ziegler investigated the optimisation of the pump control system by design measures of the system itself, like changing e.g. diameter or lever arm of the adjustment cylinder. Especially for applications within secondary controlled systems (basically velocity control) further investigations were made by Metzner (1985), Haas (1989) and Berg (1999).

Since most of earlier publications have discussed design optimisation of the mechanical part of the control system, this paper focuses on control measures achieving higher bandwidth of the pump control system. By developing a secondary controlled motor concept Berg and Ivantysynova (1999) proposed a swash plate controller of higher order for the inner control loop of a cascaded control structure. With this concept they achieved a bandwidth of 80 Hz of the pump control system for measured frequency response for 10% amplitude of commanded swash plate angle. Also Bahr Khalil et al (2002) successfully improved response dynamics of a servo pump swash plate actuation system using PD design for the swash plate controller.

3 Mathematical Model of the Pump Control System

Figure 3 shows a typical arrangement of an electro-hydraulic pump control system. The servo valve (1) controls the oil flow to and from the pump control

cylinder (2), which is mechanically linked to the swash plate (3). A deflection of the swash plate out of its centred position in either direction increases the stroke of the pistons (5) and therefore the displacement volume of the pump. The direction of deflection defines the flow direction for given direction of shaft speed. In some designs, a centring spring (6) is used to create a centring force onto the pump control cylinder whenever it is deflected from its centred position. This force will centre the swash plate when the pressure supply for the pump control system fails. Since a centring spring has no significant effect to the controller design procedure, it will not be considered for further analysis. It should be mentioned here that for the majority of variable displacement pumps the flow rate of the pump control system is relatively low. Thus the flow forces are very small and consequently the use of single stage servo valves with an electric linear motor driving the valve spool directly is a good choice, refer Fig. 4. In case of lower dynamic performance requirements proportional valves without any pilot valve can also be used.

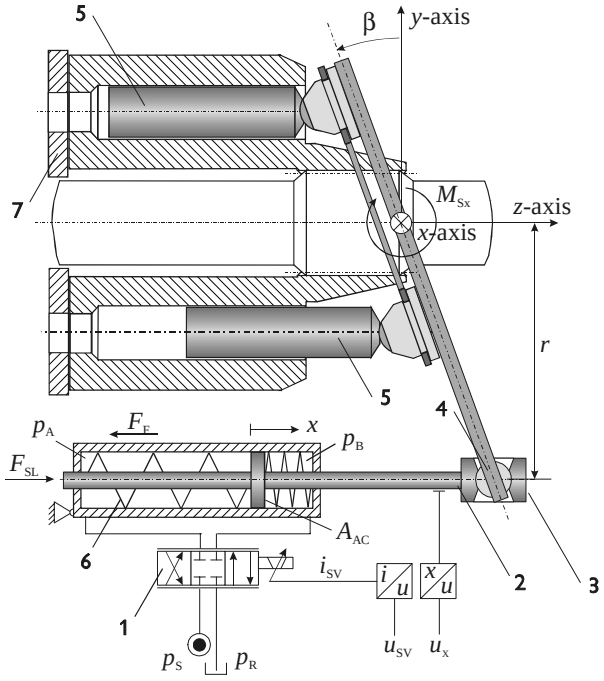

Fig. 3: *Servo pump control system*

The basic dynamic model of the pump control system – before performing further dominance analysis – is based upon the equation of motion for the pump control cylinder, the pressure build-up equations for both chambers of the cylinder, including the volume of the connecting lines between the cylinder and the pump control valve, and the equation of motion for the control valve.

For the balance of forces the inertia of all moveable parts (the swash plate, the pistons and the pump control cylinder) can be reduced to an equivalent mass, using the equivalency of rotational and translatory energy. All forces act directly on the control cylinder (see Fig. 4). The coordinates are defined achieving that a positive deflection of the servo valve spool y (to the left) results in a positive motion of the pump control cylinder x (to the right) and a positive pump flow. A linear electric motor serves as electro-mechanical converter here.

For the simplified model of Fig. 4 the equation of motion of the cylinder gives

$$m_{\text{equ}} \cdot \ddot{x} = F_{\Delta\text{p}} - F_{\text{F}} - F_{\text{SL}} , \tag{1}$$

where $$F_{\Delta p} = A_{\text{AC}} \cdot (p_{\text{A}} - p_{\text{B}}) = A_{\text{AC}} \cdot \Delta p . \tag{2}$$

The friction force F_{F} is given by a Stribeck model:

$$F_{\text{F}} = \underbrace{f_{\text{C}}\,\text{sign}(\dot{x})}_{\textit{Coulomb}} + \underbrace{f_{\text{v}}\dot{x}}_{\textit{viscous}} + \underbrace{f_{\text{s}} e^{-\tau_{\text{s}}|\dot{x}|}\,\text{sign}(\dot{x})}_{\textit{static}} \tag{3}$$

The self adjusting force F_{SL} are the forces that act on the pump control cylinder due to the piston forces applied on the swash plate and generating a moment M_{Sx} about x – axis of the swash plate, see Fig. 3. The swash plate moment M_{Sx} depends on system pressure, shaft speed, piston friction forces, viscosity, temperature, and swash plate angle. It is mainly influenced by the valve plate design and the resulting instantaneous cylinder pressure p_{i}. A simplified analytical approach to calculate the swash plate moment M_{Sx} can be found in Ivantysyn and Ivantysynova, (2000), where only pressure forces applied on the individual pistons are taken into account:

$$M_{\text{Sx}} = \frac{R}{\cos^2\beta} \sum_{i=1}^{z} A_{\text{Piston}} \cdot (p_{\text{e}} - p_{\text{i}}) \cdot \cos\varphi_{\text{i}} \tag{4}$$

The self adjusting force F_{SL} can then be obtained by

$$F_{\text{SL}} = \frac{M_{\text{Sx}}}{r} \tag{5}$$

It should be mentioned here that a much more precise determination of the swash plate moment M_{Sx} can be obtained by the multi-domain simulation tool CASPAR, which has been developed in the research group of the authors as special design tool for swash plate axial piston machines, see Wieczorek and Ivantysynova (2002) and Ivantysynova et.al. (2002). CASPAR allows the calculation of oscillating forces applied on the swash plate considering the instantaneous cylinder pressure in each piston chamber and all other forces applied on each piston/slipper assembly including the viscous friction forces resulting from real gap heights. The gap heights are calculated considering the micro-motion of parts leading to higher frequency of pulsating forces than given by the basic kinematic relationship of the pump.

The pressure build-up inside each cylinder chamber of the pump control cylinder is determined by:

$$V_{\text{A}} \cdot \dot{p}_{\text{A}} = K_{\text{Oil}} \left(Q_{\text{A}} - A_{\text{AC}}\dot{x} - k_{\text{LA}} p_{\text{A}} - k_{\text{Li}} (p_{\text{A}} - p_{\text{B}}) \right), \tag{6}$$

$$V_{\text{B}} \cdot \dot{p}_{\text{B}} = K_{\text{Oil}} \left(Q_{\text{B}} - A_{\text{AC}}\dot{x} - k_{\text{LB}} p_{\text{B}} - k_{\text{Li}} (p_{\text{B}} - p_{\text{A}}) \right) \tag{7}$$

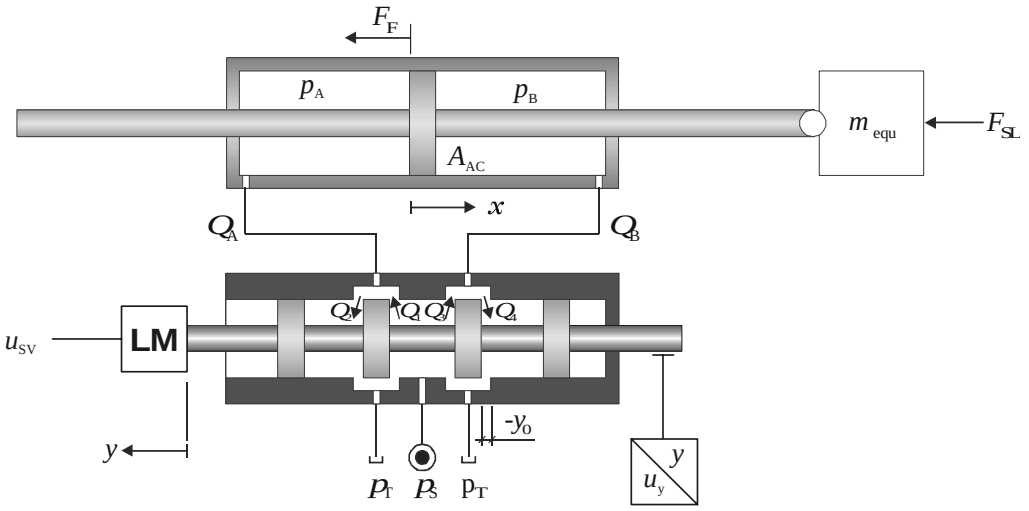

Fig. 4: *Simplified model of the servo pump control system*

The cylinder chamber volumes are calculated from the current cylinder position x in relation to the middle position x_H. Additionally, the dead volume of the connections is considered:

$$V_A = V_{dead} + A_{AC}(x_H - x) \tag{8}$$

and

$$V_B = V_{dead} + A_{AC}(x_H + x) \tag{9}$$

The hydraulic capacitance is given by the ratio of chamber volume and bulk modulus. For hydraulic capacitance of both chambers follows:

$$C_{H,A} = \frac{V_A}{K_{Oil}} \quad \text{and} \quad C_{H,B} = \frac{V_B}{K_{Oil}}. \tag{10}$$

The common hydraulic capacitance of both chambers yields

$$\begin{aligned} C_H &= \frac{1}{K_{Oil}}\left(\frac{1}{V_A}+\frac{1}{V_B}\right)^{-1} \\ &= \frac{1}{K_{Oil}}\left(\frac{A_{AC}x_H + V_{dead}}{2} + \frac{A_{AC}^2 x^2}{2(A_{AC}x_H + V_{dead})}\right) \end{aligned}. \tag{11}$$

For a servo valve with zero overlap ($y_0 = 0$) the volume flow of the servo valve yields:

$$Q_A = \begin{cases} B \cdot y\sqrt{|\,p_S - p_A\,|}\,\mathrm{sign}(p_S - p_A) & \text{for } y \geq 0 \\ B \cdot y\sqrt{|\,p_A - p_R\,|}\,\mathrm{sign}(p_A - p_R) & \text{for } y < 0 \end{cases} \tag{12}$$

and

$$Q_B = \begin{cases} B \cdot y\sqrt{|\,p_B - p_R\,|}\,\mathrm{sign}(p_B - p_R) & \text{for } y \geq 0 \\ B \cdot y\sqrt{|\,p_S - p_B\,|}\,\mathrm{sign}(p_S - p_B) & \text{for } y < 0 \end{cases} \tag{13}$$

Assuming, that $Q_A = Q_B$ both equations give the following simplification:

$$Q_{SV} = Q_A = Q_B = B \cdot y\sqrt{\frac{|\,p_S - \Delta p\,|}{2}}\,sign\left(p_S - \Delta p\,sign(y)\right) \tag{14}$$

using $\Delta p = p_A - p_B$ as the differential pressure of the pump control and assuming the reservoir pressure to be $p_R \approx 0$ bar. The equations for the pressure build-up can then be transformed to

$$\dot{p}_A = \frac{1}{C_{H,A}}\left(Q_A - A_{AC}\dot{x} - k_{LA}p_A - k_{Li}(p_A - p_B)\right) \tag{15}$$

and

$$\dot{p}_B = \frac{1}{C_{H,B}}\left(Q_B + A_{AC}\dot{x} - k_{LB}p_B + k_{Li}(p_A - p_B)\right) \tag{16}$$

For further simplification the pressure equations can be transformed to differential pressure, using

$$\Delta p = p_A - p_B \text{ and } Q_A = -Q_B, \tag{17}$$

where the external leakages have been neglected:

$$\Delta\dot{p} = \frac{1}{C_H}(Q_A - A_{AC}\dot{x} - k_{Li}\Delta p) \tag{18}$$

The state space equation follows from Eq. 1 to Eq. 18:

$$\begin{aligned} \dot{x}_1 = \Delta\dot{p} &= -\frac{A_{AC}}{C_H}\dot{x} + \frac{B}{C_H}y\sqrt{\frac{p_S - \Delta p}{2}} - \frac{k_{Li}\Delta p}{C_H} \\ \dot{x}_2 &= x_3, \\ \dot{x}_3 &= \frac{1}{m_{equ}}(A_{AC}\Delta p - F_F - F_{SL}) \end{aligned} \tag{19}$$

using the state vector $\mathbf{x} = \begin{bmatrix} \Delta p_{VK} \\ x \\ \dot{x} \end{bmatrix}$ (20)

The dynamic behaviour of the servo valve depends on a large number of design and operating parameters and a detailed mathematical model based on a description of all physical effects would require a large number of detailed design parameters, which are very often not available for the system engineer. The valve dynamics can be with sufficiently high precision modelled by approximation of measured step or frequency responses. The valve dynamics can be described by a second order system. Figure 5 shows a typical shape of a frequency response characteristic of a servo valve. The nonlinear behaviour of the system is obvious. Assuming a second order system (PT_2 system) for descrip-

tion of the dynamic behaviour of the electro-mechanical converter and the spool movement, i.e. the transfer function between valve input signal and spool movement, the dynamics of the servo valve of the pump controlled system yields:

$$\ddot{y} + 2d_{SV}\omega_{SV}\dot{y} + \omega_{SV}{}^2 y = k_{SV}\omega_{SV}{}^2 u_{SV} \tag{21}$$

$$G(s) = \frac{k_{SV}}{\frac{1}{\omega_{SV}^2}s^2 + 2\frac{d_{SV}}{\omega_{SV}}s + 1}u_{SV} \tag{22}$$

where the valve gain is $k_{SV} = y_{SV,\,max}/u_{SV,\,max}$. However, by looking at typical Bode diagrams of servo valve dynamics, e.g. as shown in Fig. 5, the nonlinear behaviour of the valve is obvious.

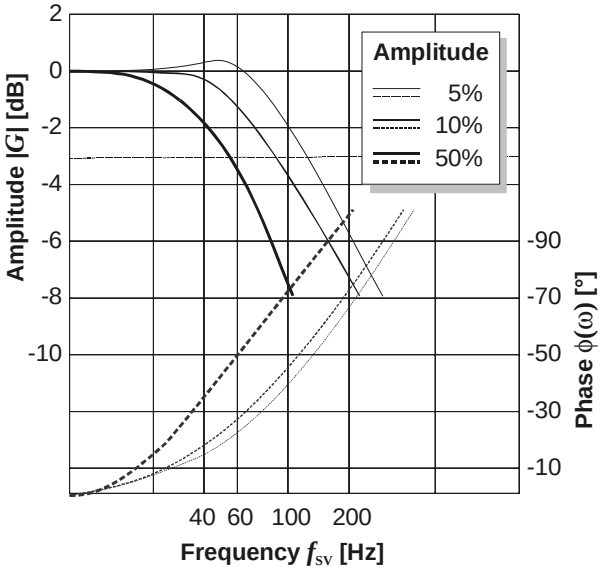

Fig. 5: *Servo valve frequency response*

Consequently, the PT_2 characteristics of a servo valve, given by the eigenfrequency ω_{SV} and the damping coefficient d_{SV}, maybe considered as non-linear parameters (uncertainties). Figure 6 shows the block diagram of the non-linear model of the pump control system, which is explained in this chapter.

Linearized Model

For a controller design method based upon a linear plant model all remaining non-linearities need to be linearized around a suitable operating point. Therefore, the middle position of the pump control cylinder was chosen. Since the load pressure and the effective inertia are quite low compared to other valve controlled cylinder applications, this operating point appears to be reasonable. The hydraulic capacitance C_H is then fixed at the centred position:

$$C_{H,\,A} = C_{H,\,B} = C_H = C_H|_{x\,=\,x0}. \tag{23}$$

For the servo valve flow Q_{SV} linearization a Taylor series is required. The 1st order approximation of Eq. 14 yields:

$$Q_{SV} = \left.\frac{\partial Q_{SV}}{\partial y}\right|_{\Delta pOP} \cdot y + \left.\frac{\partial Q_{SV}}{\partial \Delta p}\right|_{\Delta yOP} \cdot \Delta p \tag{24}$$
$$Q_{SV} = C_y \cdot y + C_p \cdot \Delta p$$

The coefficients C_y (volume flow amplification) and C_p (pressure amplification) are calculated to:

$$C_y = B\sqrt{\frac{p_s - \Delta p_{OP} \cdot sign(y_{OP})}{2}} = \frac{Q_{SV,max}}{y_{max}}\sqrt{1 - \frac{\Delta p_{OP}}{p_V} \cdot sign(y_{OP})} \tag{25}$$

$$C_p = -\frac{B \cdot y_{OP}}{4\sqrt{2(p_S - \Delta p_{OP} sign(y_{OP})}}$$

and

$$= -\frac{Q_{max} \cdot y_{OP}}{2(p_{SR} y_{max}\sqrt{1 - \frac{\Delta p_{OP}}{p_V} \cdot sign(y_{OP})}} \tag{26}$$

Applying the above mentioned assumptions for the operating point, this yields

$$C_y = B\sqrt{\frac{p_S - \Delta p_{OP} \cdot \mathrm{sign}(y_{OP})}{2}}\Bigg|_{y_{OP}=0,\ \Delta p_{OP}=0} = B\sqrt{\frac{\Delta p_S}{2}} \tag{27}$$

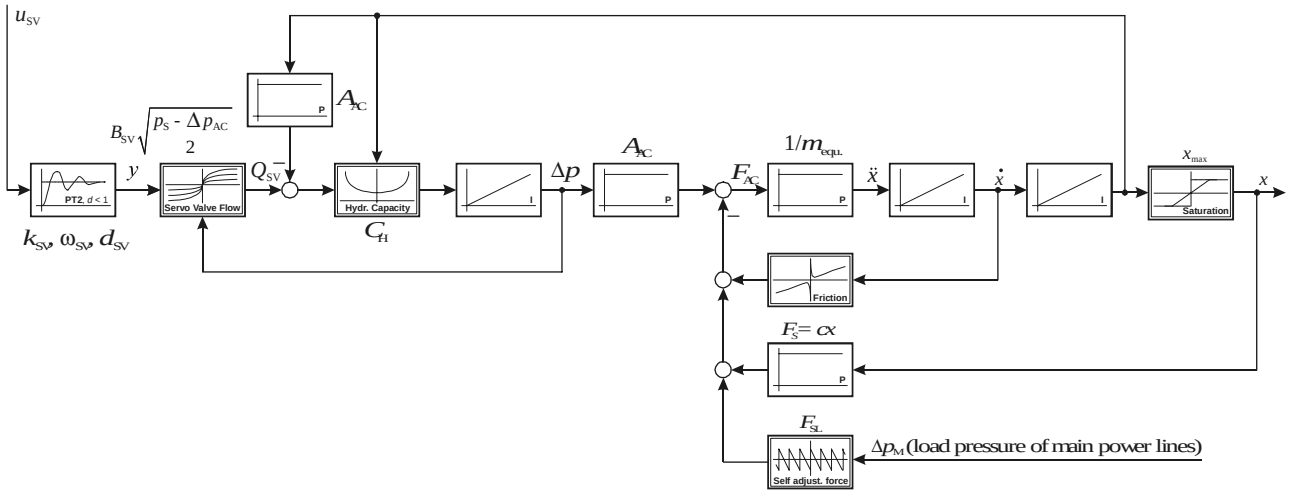

Fig. 6: *Servo pump adjustment system*

$$C_p = \left.\frac{B \cdot y_{OP}}{4\sqrt{2(p_s - \Delta p_{OP}\mathrm{sign}(y_{OP})}}\right|_{y_{OP}=0,\Delta p_{OP}=0} = 0 \qquad (28)$$

It should be noted that the model reduction, resulting from neglecting the load force, and thus C_p, is only acceptable for the low pay-loads, found here. In other cases it might be useful to linearize C_p around an operating point with average load pressure.

A linearization of the friction force F_F can only cover for viscous friction, which is linearly dependent on the velocity of the pump control cylinder. The remaining terms (static friction and Coulomb friction) need to be treated as disturbance force:

$$F_{F,\mathrm{lin}} = f_v \cdot \dot{x}\,. \qquad (29)$$

Finally, the linearized state space model yields

$$\dot{x}_1 = \Delta\dot{p} = -\frac{A_{AC}}{C_{H,}}\dot{x} - \frac{k_{Li}}{C_H}\Delta p + \frac{C_y}{C_H}y$$

$$\dot{x}_2 = x_3 \qquad (30)$$

$$\dot{x}_3 = \ddot{x} = \frac{A_{AC}}{m_{equ}}\Delta p_{AC} - \frac{f_v}{m_{equ}}\dot{x}$$

Consequently, the matrices of the linearized system yield:

$$\mathbf{A} = \begin{bmatrix} \frac{k_{Li}}{C_H} & 0 & -\frac{A_{AC}}{C_H} \\ 0 & 0 & 1 \\ \frac{A_{AC}}{m_{equ}} & 0 & -\frac{f_v}{m_{equ}} \end{bmatrix}; \mathbf{B} = \begin{bmatrix} \frac{C_y}{C_H} \\ 0 \\ 0 \end{bmatrix}; \qquad (31)$$

$$\mathbf{C} = \begin{bmatrix} 0 & 1 & 0 \end{bmatrix}; \mathbf{D} = 0$$

The transfer function can be derived from the state space model:

$$G(s) = \mathbf{C}^T \cdot (s \cdot \mathbf{I} - \mathbf{A})^{-1} \cdot \mathbf{B} + \mathbf{D}$$

$$= \frac{A_{AC}C_y}{m_{equ}C_H s^2 + (f_v C_H + k_{Li} m_{equ})s + A_{AC}^2 + k_{Li} f_v} \cdot \frac{1}{s} \qquad (32)$$

This transfer function is divided into a second order function (left) and an integrator (right). The second order function can be transferred into oscillator writing:

$$G(s) = \frac{1}{s} \cdot \frac{\frac{A_{AC}C_y}{A_{AC}^2 + k_{Li} f_v}}{\frac{m_{equ}C_H}{A_{AC}^2 + k_{Li} f_v}s^2 + \frac{k_{Li}m_{equ} + f_v C_H}{A_{AC}^2 + k_{Li} f_v}s + 1} \qquad (33)$$

$$= \frac{1}{s} \cdot \frac{k_{AC}}{\frac{1}{\omega_{AC}^{\ 2}}s^2 + \frac{2d_{AC}}{\omega_{AC}}s + 1}$$

with the hydraulic eigenfrequency of the pump control system

$$\omega_{SV} = \sqrt{\frac{A_{AC}^{\ 2} + k_{Li} f_v}{m_{equ}C_H}} \qquad (34)$$

damping

$$d_{AC} = \frac{f_v C_H + k_{LI} m_{equ}}{2\sqrt{m_{equ}C_H(A_{AC}^{\ 2} + k_{Li} f_v)}} \qquad (35)$$

and hydraulic system gain

$$k_{AC} = \frac{A_{AC} \cdot C_y}{A_{AC}^{\ 2} + k_{Li} \cdot f_v} \qquad (36)$$

The corresponding eigenvalues yield:

$$p_0 = 0; \qquad (37)$$

$$p_{1,2} = \frac{C_H f_v - k_{Li} m_{equ}}{2m_{equ}C_{H,\,AC}} \pm \sqrt{\left(\frac{f_v C_H + k_{Li} m_{equ}}{2m_{equ}C_H}\right)^2 - \frac{k_{Li} f_v}{m_{equ}C_H} - \frac{A_{AC}^{\ 2}}{m_{equ}C_H}} \qquad (38)$$

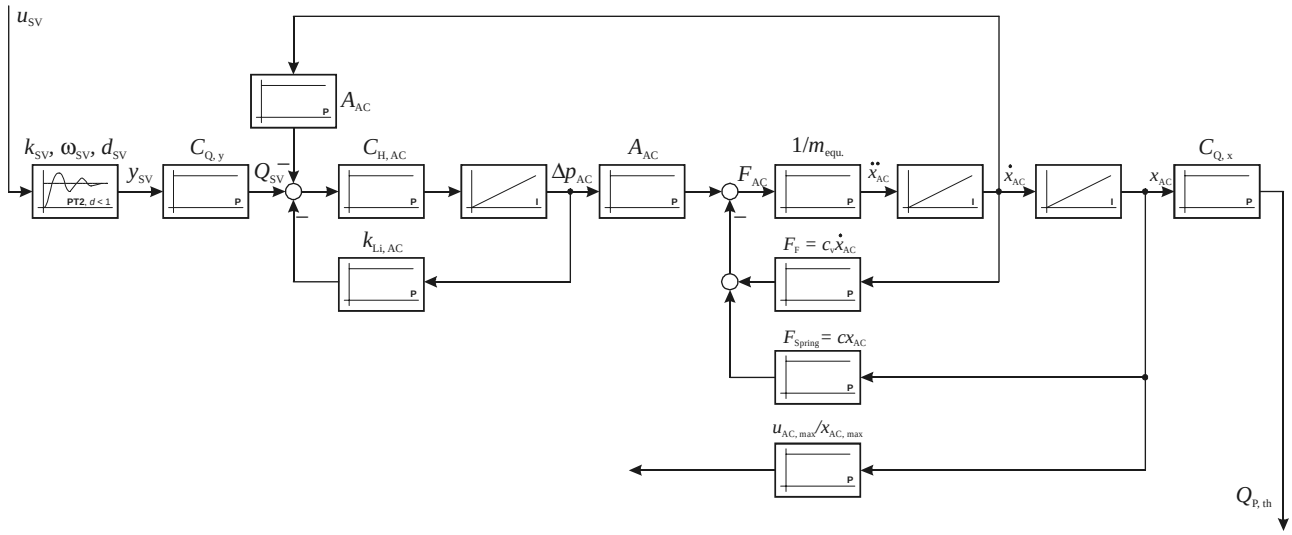

Fig. 7: *Linearized model of the servo pump control system*

When the loss terms are neglected (since they basically influence the damping and have very little influence on the eigenfrequency) the result for the eigenfrequency can be simplified to:

$$\omega_{AC} = \sqrt{\frac{A_{AC}^{\ 2}}{m_{equ} C_H}} \tag{39}$$

The block diagram of the simplified system is shown in Fig. 7.

4 Dominance Analysis

In order to estimate the servo pump dynamics, it is required to estimate size and volume intervals of typical pump control cylinder designs. Since this study is focussed on industrially available components, the design parameters are taken from typical pump dimensions. However, further geometric optimisation of the pump control system may result in smaller cylinder sizes and thus further improved dynamics (that requires higher pump control system supply pressure on the other hand). For deriving the hydraulic eigenfrequency of the servo pump control cylinder, we recall Eq. 39 and see, that ω_{AC} gets minimized, when $C_{H,\,AC}$ is maximized, what is, according to Eq. 11, when $x = x_H$. This yields

$$C_{H,\max} = \frac{A_{AC} x_H}{K_{Oil}} \tag{40}$$

and

$$\omega_{AC,\min} = \sqrt{\frac{K_{Oil} A_{AC}}{m_{equ} x_H}} \tag{41}$$

For the pump control cylinder the following parameter ranges are assumed (according to existing pump designs of different manufacturers in a range of approx. 10 to 250 cm³/rev):

- a cylinder stroke of x_H = 5 .. 20 mm,
- a cylinder diameter of d_{AC} = 10 .. 50 mm,
- an equivalent mass of m_{equ} = 0.2 .. 1 kg and
- a range for $K_{Oil} = 1.6 \;..\; 3.2 \cdot 10^9 \,\frac{\mathrm{N}}{\mathrm{m}^2}$

This results in an expected eigenfrequency range of the pump control cylinder (also hydraulic eigenfrequency of the system) of

$$\omega_{AC} = 2\,500 \;..\; 80\,000 \text{ rad/s}$$

equiv. to f_{AC} = 400 .. 12 600 Hz. (42)

A quite important fact should be pointed out from Eq. 42. Assuming a linear scaling of an existing pump design, that increases all lengths by factor 2, all areas by factor 4 and all masses and volumes by factor 8, we can see that the numerator of the term below the root of Eq. 41 will increase by factor 4 (area A_{AC}), while the denominator will increase by factor 16 (mass m_{equ} and stroke x_H), resulting a *reduction* of the eigenfrequency ω_{AC} of the adjustment cylinder itself by the *linear* scaling factor of 2. In other words: a servo pump with a displacement volume 8 times bigger will lead to only half the hydraulic eigenfrequency of the pump control cylinder.

Assuming further, that standard single stage servo valves using a linear motor as electro-mechanical converter are applied we can consider a valve eigenfrequency range of about

$$\omega_{SV} \approx 500 \;..\; 750 \text{ rad/s},$$

equiv. to $f_{SV} \approx 80 \;..\; 120$ Hz (43)

Hence, the poles of the servo valve will always dominate the pump control system open-loop characteristics, especially, when considering, that typically smaller (= faster) valves are uses with smaller (= faster) pumps:

$$\omega_{AC} >> \omega_{SV} \tag{44}$$

The consequence of this relation is very important. In contrast to all typical hydraulic drives used in heavy duty machinery, where the hydraulic eigenfrequency and the natural damping of the hydraulic circuit dominates the system behavior, here the eigenfrequency and damping of the control valve dominate the system characteristics. This means that typical control approaches used for typical valve controller design approaches for hydraulic machinery cannot be used here.

Summarizing, the complete pump control system dynamics are then reduced to the following equations:

Servo valve:

$$\ddot{y}_{SV} + 2 d_{SV} \omega_{SV} \dot{y}_{SV} + \omega_{SV}^{\ 2} y_{SV} = k_{SV} \omega_{SV}^{\ 2} u_{SV} \tag{45}$$

Valve flow: $Q_{SV} = C_y \cdot y_{SV}$ (46)

Cylinder velocity: $\dot{x} = \frac{Q_{SV}}{A_{AC}}$ (47)

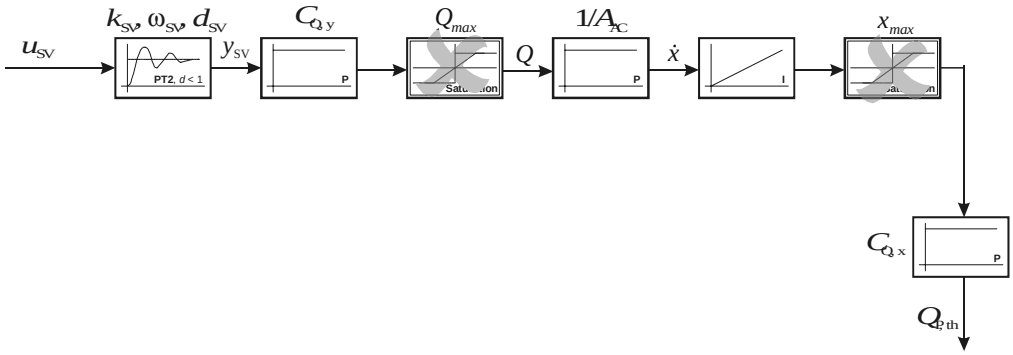

Fig. 8: *Simplified model of the servo pump control system*

The block diagram for this simplified model is shown in Fig. 8. The crossed blocks illustrate remaining system saturations that need to be removed for a pure linear model. The transfer function for the complete pump control system is then reduced to a third order system, that represents the required parameters:

$$G_{\mathrm{AS,open}}(s) = \frac{1}{s} \cdot \frac{C_\gamma}{A_{\mathrm{AC}}} \cdot \frac{k_{\mathrm{sv}}}{\frac{1}{\omega_{\mathrm{sv}}} \cdot s^2 + 2 \cdot \frac{d_{\mathrm{sv}}}{\omega_{\mathrm{sv}}} \cdot s + 1} \qquad (48)$$

Further, this simplification means, that all parameters influencing the location of the hydraulic poles can be neglected:

- The bulk modulus K_{oil}
- The chamber volumes V_{A} and V_{B}
- The friction force F_{F}
- The leakage flow Q_{L}
- Effective inertia of the pump control system Θ_{AS}.

Not to be misunderstood, this does not mean, that these parameters are irrelevant. It does mean that, once the system is designed to achieve sufficient forces to overcome the swash plate moment and centring spring forces (when applicable), the *controller design* does not rely on these parameters.

The design of the pump control systems and especially the cylinder geometry must, however, take the following forces into account, which have to be surpassed at all operating conditions:

- Self adjusting force F_{SL} due to the swash plate moment M_{Sx}: The design of the control system has to ensure, that this force is surpassed at all operating conditions. The effective characteristic of this force needs to be measured or calculated. In case that the system should be designed in an optimised way, the dependency of the real swash plate moment M_{Sx} on operating parameters (pressure, speed and swash plate angle) must be considered (e.g. using CASPAR).
- The friction force F_{F} of the pump control system is acting in opposite direction to the piston motion of the pump control cylinder and has to be surpassed by the acting pressure force.
- For safety reasons the pump control system can be provided with an additional centring spring which forces the swash plate to a neutral position in case the pressure supply of the pump control system fails. A centring effect can also be realized by an appropriate swash plate design.

By summing all forces acting on the swash plate (pressure force of the adjustment cylinder, friction force, self adjusting force and centering spring force), the effective inertia of the moved parts will define the maximum acceleration of the swash plate (the *actuation velocity* is however, finally limited by the servo valve flow characteristic).

It can be stated, that although these forces will define the final geometry of the pump control cylinder and consequently cause the velocity saturation of the pump control system (in conjunction with the servo valve flow constant B and the pressure supply level p_{S}), they will neither effect the final dynamics of the pump control systems nor its controller structure.

Consequently, the open loop characteristics of the servo pump control system are dominated by the dynamics of the servo valve used (ω_{SV}, d_{SV}, k_{SV}) and the gain of the pump control system k_{AC} (representing the pump control cylinder area A_{AC}, the servo valve flow constant B and the supply pressure p_{S}), as derived before. It was already mentioned that especially the servo valve characteristics ω_{SV} and d_{SV} vary with respect to the commanded step size. Especially for a controller design of higher order it is necessary to consider these parameters as uncertainties in order to achieve required closed loop dynamics at any operating point and thus at any step command. Therefore, the parameter space method developed by Ackermann (1993) was used. It is necessary to briefly introduce this method and its controller design procedure.

5 The Parameter Space Approach

The term “robust control” relates to the control of plants with uncertain parameters and uncertain disturbances. The design problem is to find a controller with fixed parameters that achieves acceptable dynamic behaviour for the controlled plant at all operating points. A number of different design approaches are known from literature, like the μ-synthesis or the Ackermann parameter space method. Especially the latter appears suitable for the design problem given here due to its straightforward approach.

The parameter space method is a design method for calculating the controller parameters of a fixed parameter regulator of any kind at a given linear plant structure, where the uncertainties are defined as parameter intervals with lower and upper boundaries. The design approach allows defining a target region for the poles of the controlled closed loop system that fulfils the desired restrictions on their location (as eigenfrequency and damping). This region is referred to as “Γ-region”.

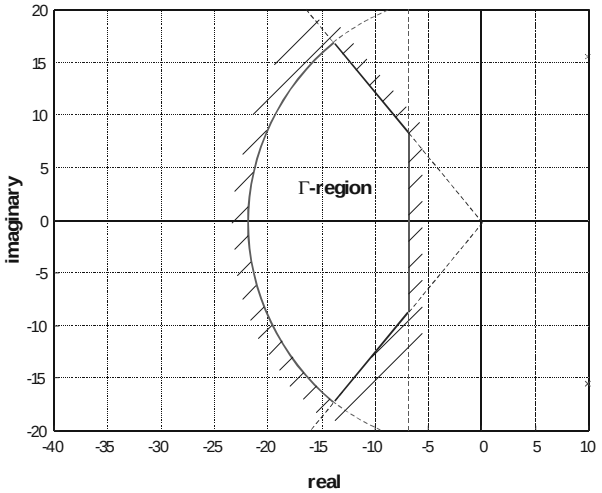

Fig. 9: *Example of a Γ-region*

A system is called “Γ-stable”, when all poles of the closed loop system are located inside the defined “Γ-

region". A system is called "robust Γ-stable", when all poles of the closed loop system are located inside the defined "Γ-region" for all given operating points. A typical example for a Γ-region is shown in . However, it is not necessary for the approach to have a single connected region, also a number of unconnected regions can be defined as Γ-region.

The controller design of the parameter space method is done consecutively by carrying out the following steps:

- For a linear state space model describing the plant structure a number of operating points are defined to represent all necessary system operating conditions. For each operating point the uncertain parameters are fixed to their current value, giving upper and lower borders for all uncertain parameters. The regulator structure is defined (and thus not result of the design process), where the regulator parameters k_1 .. k_n are the $\frac{n}{2}$ coefficients to be calculated during the parameter space design process.
- Transformation of the Γ-region from the s-plane into the *k*-space (parameter space) for all k_i (Fig. 10). The cross section or cross-space, respectively, is the area for which all k_i inside fulfil the demands defined by the Γ-region. This means, that any combination of regulator parameters k_i from the cross-area brings the closed loop poles into the defined Γ-region for all given operating points.
- Since the design process only takes discrete operating points into consideration, it needs to be verified that all other operating points are inside the area or space defined by the parameter intervals. If this is not the case, additional operating points need to be defined and the design process has to be repeated.

6 Uncertain Parameters of the Pump Control System

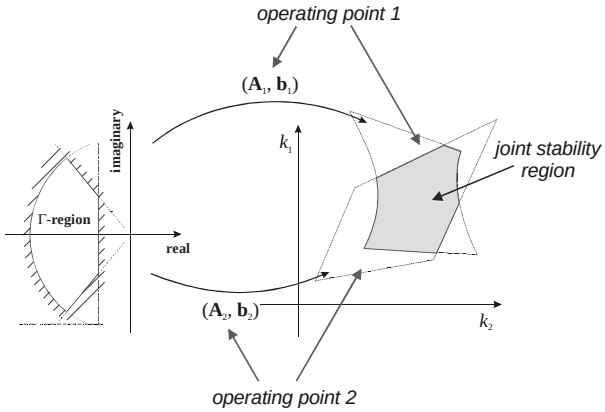

Fig. 10: *Transformation scheme*

It can be assumed that the geometry of the servo pump control system, especially the diameter, stroke and lever arm of the pump control cylinder, is known and not subject to plant uncertainties. Further it was shown, that the design parameters of the pump control system other than servo valve dynamics are not dominant for the system dynamics.

The remaining uncertainties are eigenfrequency ω_{SV} and damping d_{SV} of the servo valve. These are also the only relevant uncertainties with respect to the dominance analysis. It has to be noted, that all parameter space uncertainty investigations need to be done numerically. However, since for electro-hydraulic pump control system single-stage servo valves of high response dynamics should be preferred today, a reasonable assumption for the servo valve dynamics (see also section "Dominance Analysis" further above) is stated as

$$\omega_{SV} = 400 \text{ .. } 600 \text{ rad/s} \approx 65 \text{ .. } 95 \text{ Hz}$$

and $$d_{SV} = 0.7 \text{ .. } 1.0 \qquad (49)$$

The nominal parameters are given by

$$\omega_{SV} = 500 \text{ rad/s} \approx 80 \text{ Hz}$$

and $$d_{SV} = 0.8$$

Fig. 11 shows the area (shaded in grey) of the uncertain poles of the servo valve in the *s*-plane.

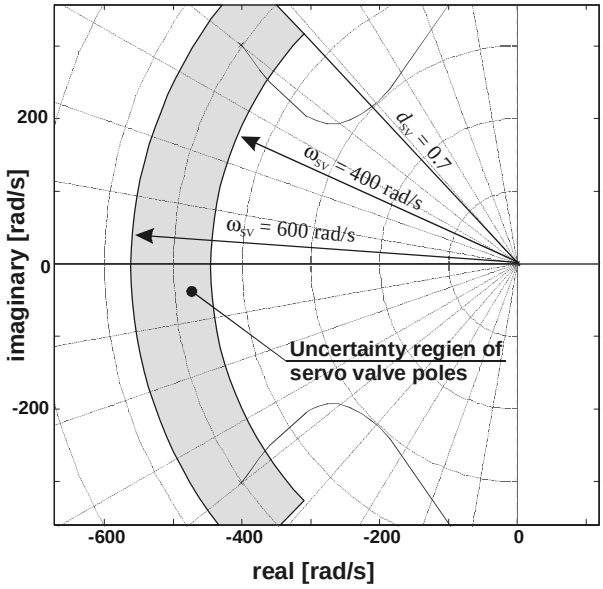

Fig. 11: *Region of uncertain parameters of the servo valve*

6.1 Proportional Control

The logical first approach for an open-loop plant of the derived characteristics (domination of a sufficiently damped pole pair, integrative behaviour of the open-loop plant) is proportional control, which is also the standard design known from literature (since most servo pump control systems are still based upon simple analogue control logic electronics). Consequently, the regulator transfer function for this type of control yields

$$K_{SPC}(s) = k_{SPC} \,. \qquad (50)$$

Fig. 13 shows the block diagram of the controlled swash plate position of the servo pump, using the simplified model of the pump control system.

For the simplified structure of the pump control system the state space model gives

$$\mathbf{A}_{\mathrm{AS}} = \begin{bmatrix} 0 & 1 & 0 \\ -\omega_{\mathrm{SV}}{}^2 & -\omega_{\mathrm{SV}} d_{\mathrm{SV}} & 0 \\ C_{\mathrm{y}} / A_{\mathrm{AC}} & 0 & 0 \end{bmatrix}; \; \mathbf{b}_{\mathrm{AS}} = \begin{bmatrix} 0 \\ k_{\mathrm{SV}} \cdot \omega_{\mathrm{SV}}{}^2 \\ 0 \end{bmatrix};$$

$$\mathbf{c}_{\mathrm{AS}}{}^T = \begin{bmatrix} 0 & 0 & \dfrac{u_{\mathrm{SV,max}}}{x_{\max}} \end{bmatrix}; \; d = 0 \qquad (51)$$

using the state vector $\mathbf{x}_{\mathrm{AS}} = \begin{bmatrix} y \\ \dot{y} \\ x \end{bmatrix}$, (52)

the input $\mathbf{u} = u_{\mathrm{SV}}$ and the ouput $y = u_{\mathrm{x}}$.

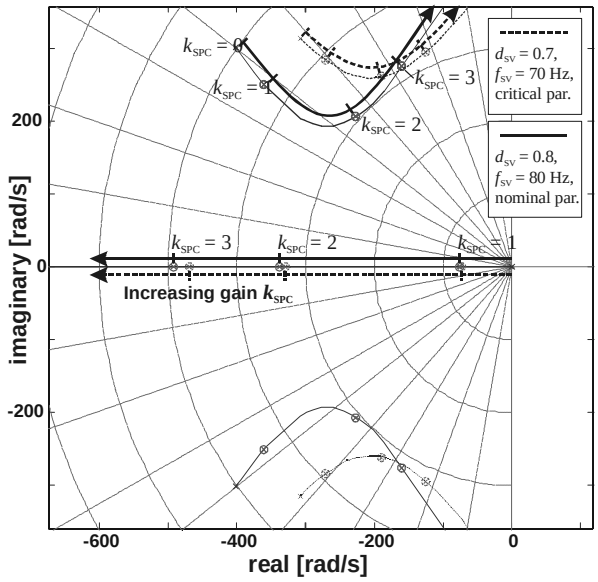

Fig. 12: *Pole trajectories of the plant for proportional control, shown at nominal parameters of the servo valve*

The only free parameter in the controller design to tune the system (apart from hardware changes, of course) is the forward gain k_{SPC} of the regulator. Figure 12 shows the pole trajectories of the P-controlled servo pump control system according to the block diagram shown in Fig. 13 for nominal parameters for the servo valve (ω_{SV} = 500 rad/s, d_{SV} = 0.8) and for a parameter combination, that appears most critical with respect to the stability margin (minimum eigenfrequency $\omega_{\mathrm{SV}} = \omega_{\mathrm{SV,\,min}}$ = 400 rad/s and minimum damping $d_{\mathrm{SV}} = d_{\mathrm{SV,\,min}}$ = 0.7).

This combination appears to be the most critical, because here the closed loop looses stability earlier with increasing forward gain than at other combination, since the open-loop poles are already at their closest position to the imaginary axis. The figure illustrates, that

- a P-controller will be able to provide sufficient damping to the dominant pole pair of the *closed loop* as long as the forward gain k_{SPC} is not tuned too high in terms of acceptable damping for the closed loop system;
- the servo valve poles move to lower damping and towards the right *s*-plane with increasing forward gain k_{SPC};
- for lower damping d_{SV} and lower eigenfrequencies ω_{SV} of the servo valve (dashed curves) the critical gain k_{SPC} (where the closed-loop poles reach the border for critical damping) is lower than for higher damping or higher eigenfrequencies. This means, the critical situation is reached significantly earlier.

The goal of this controller design is to find the critical gain k_{SPC}, where the poles of the closed loop controlled servo pump achieve sufficient bandwidth ω_{CP} and damping d_{CP}. The parameter space design will help to find the critical gain k_{SPC} for the given parameter uncertainties.

First, the desired region for the closed-loop poles (the Γ-region) needs to be defined. The chosen region should provide sufficient damping (defined by a minimum damping ratio of the closed-loop poles $d_{\mathrm{CP,\,min}}$) to the position control of the swash plate by simultaneously keeping an acceptable bandwidth of the system (defined by a minimum eigenfrequency of the closed-loop poles $\varpi_{\mathrm{CP,\,min}}$). On the other hand, an upper limit for the bandwidth is reasonable to prevent the system reacting too quickly on measurement background noise. The parameters for the boundary conditions of the Γ-region were set to

$$\varpi_{\mathrm{CP,\,min}} = 100 \text{ rad/s}, \; \varpi_{\mathrm{CP,\,max}} = 1\,000 \text{ rad/s}$$

$$\text{and} \qquad d_{\mathrm{CP,\,min}} = 0.5 \qquad (53)$$

The corresponding Γ-region can be described by a hyperbola and a circle (Fig. 14):

$$\partial\Gamma_{\mathrm{Hyperbola}} = \{\sigma + j\omega \,|\, \left(\frac{\sigma}{a}\right)^2 - \left(\frac{\omega}{b}\right)^2 = 1, \;\; \omega \in [0; \;\infty]\} \qquad (54)$$

where $a|_{\omega\,=\,\min} = 100$ and $b|_{\,d\,=\,0.5} = 173.2$ and

$$\partial\Gamma_{\mathrm{Circle}} = \{\sigma + j\omega \,|\, \sigma^2 + \omega^2 = R^2, \;\; \sigma \in [-R; \;+R]\} \qquad (55)$$

where $R|_{\omega\,=\,\max} = 1\,000$.

The second step is the transformation of the Γ-region boundaries into the parameter space. Since the only free parameter is the proportional gain k_{SPC}, this would result in a one-dimensional representation of the parameter space. However, to keep the parameter space for this case more illustrative, the servo valve eigenfrequency ω_{SV} is shown on the second axis.

As a result from the transformation the region of joint robust stability for the complete range of the uncertain parameters is shaded in grey.

The maximum forward gain k_{SPC} for a proportional controller of the swash plate thus yields

$$k_{\mathrm{SPC,\,max}} \approx 1.25 \,..\, 1.45 \; V_{\mathrm{SV}}/V_{\mathrm{LVDT}} \qquad (56)$$

for the given parameter range of ω_{SV} = 400 .. 600 rad/s. It can also be seen that an improved bandwidth of the servo valve (= increased eigenfrequency range) would allow higher gains.

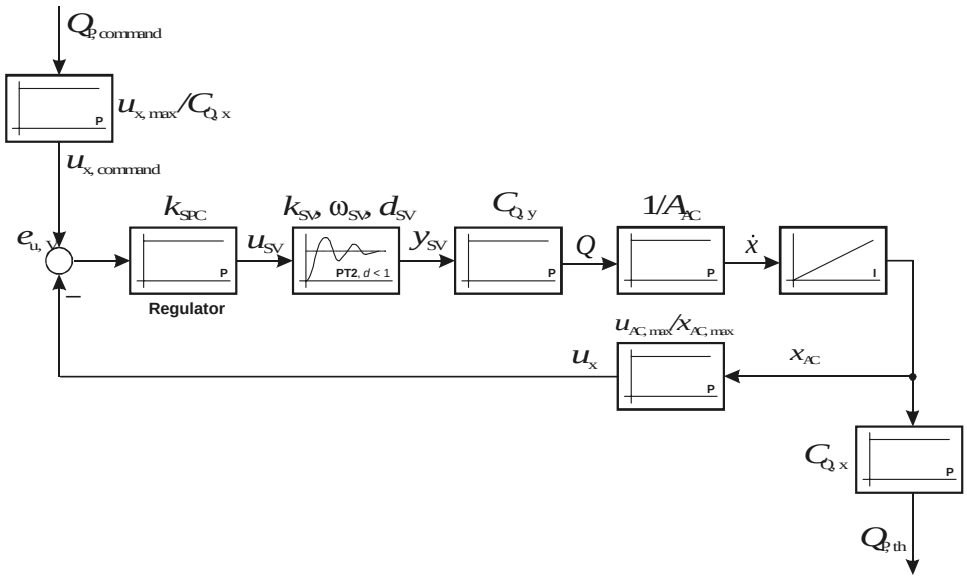

Fig. 13: *Block diagram of the controlled swash plate position*

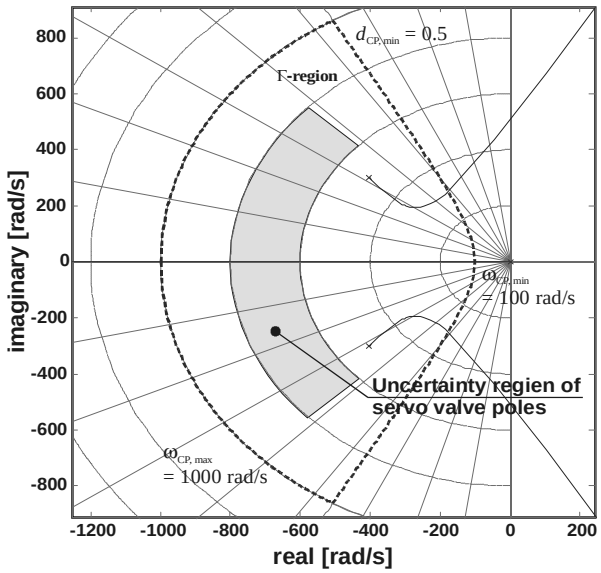

Fig. 14: *Γ-region for closed-loop poles of the swash plate control system*

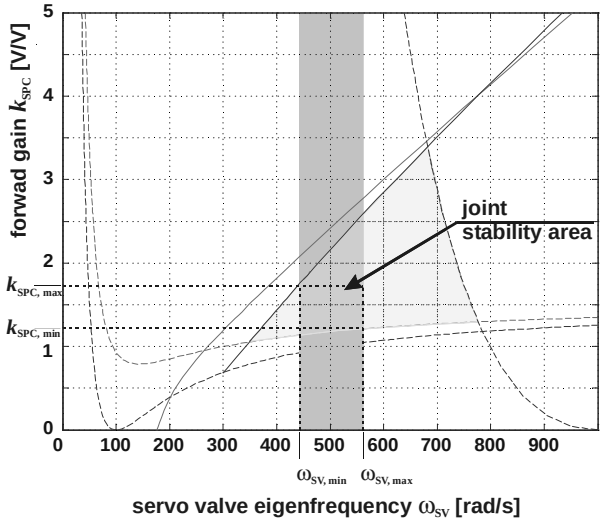

Fig. 15: *Parameter space of the proportional controller, k_{SPC} over ω_{SV}*

6.2 Second Order Forward Compensation

As the forward gain is a measure of amplification of the control error signal, the controller is acting faster on smaller error signals with increased gain, since an identical error results in a higher command signal to the servo valve. Thus, an increased forward gain basically improves the behaviour on low-level signals. On the other hand, the controller starts also acting on measurement background noise, when the forward gain is tuned too high. The bandwidth, however, is determined by the eigenfrequency of the closed-loop poles and can be considered as a measure of the time the system needs to reach a desired position.

A reasonable approach to improved swash plate controller design is to compensate the dominant servo valve dynamics by an inverse transfer function and replacing the 'cancelled' poles by a new transfer function of desired dynamics. This is provided by the following regulator transfer function:

$$K_{SPC}(s) = k_{SPC} \cdot \frac{\frac{1}{\omega_{RZ}^2}s^2 + \frac{2d_{RZ}}{\omega_{RZ}}s + 1}{\frac{1}{\omega_{RP}^2}s^2 + \frac{2d_{RP}}{\omega_{RP}}s + 1} \qquad (57)$$

Compared to proportional control this function gives five free variables to calculate during the design process:

$$k_{SPC},\ \omega_{RZ},\ d_{RZ},\ \omega_{RP} \text{ and } d_{RP}.$$

The numerator compensates the servo valve dynamics, yielding

$$\omega_{RZ} \approx \omega_{SV} \text{ and } d_{RZ} \approx d_{SV}. \qquad (58)$$

Although this approach appears logical for a system of the given characteristics, it needs to be shown by calculation as well as by test rig evaluation that it behaves as expected under all expected operating conditions, especially with respect to the changing characteristics of the servo valve as explained by Fig. (5).

But first, prior to applying the parameter space method, a parameter study for ω_{RP} and d_{RP} carried out

iteratively shows that the forward gain can further increased when using

$$d_{RP} = 1$$

and maximizing ω_{RP}:

$$\omega_{RP} \rightarrow \max$$

Fig. 16 shows the pole zero map of the swash plate controller using the controller function of Eq. 57 at nominal values for the servo valve and a forward gain of $k_{SPC} = 6$. The regulator zeros were introduced close to the nominal parameters of the servo valve, while the regulator poles were set to $d_{RP} = 1$ and $\omega_{RP} = 1200$ rad/s. The choice of ω_{RP} is limited by the Shannon theorem and the sampling frequency of the controller hardware, where the control algorithm is implemented as time discrete transfer function. The following statements can be taken from analysis of the pole zero map:

The dominant poles of the closed loop move towards the introduced regulator zeros by increasing the forward gain k_{SPC} and thus, these poles remain close to the original open-loop servo valve poles. Hereby the dominant closed-loop dynamics (ω_{CP}, d_{CP}) is shifted close to the servo valve dynamics (ω_{SV}, d_{SV}) and no longer moving closer to the imaginary axis with increased forward k_{SPC}.

At nominal servo valve parameters the forward gain k_{SPC} can be tuned approx. 4 times higher compared to proportional control, resulting in a significantly improved response behaviour in the low level signal area of command signals. However, due to *varying* servo valve dynamics the achievable forward gain is subject to a robust controller design.

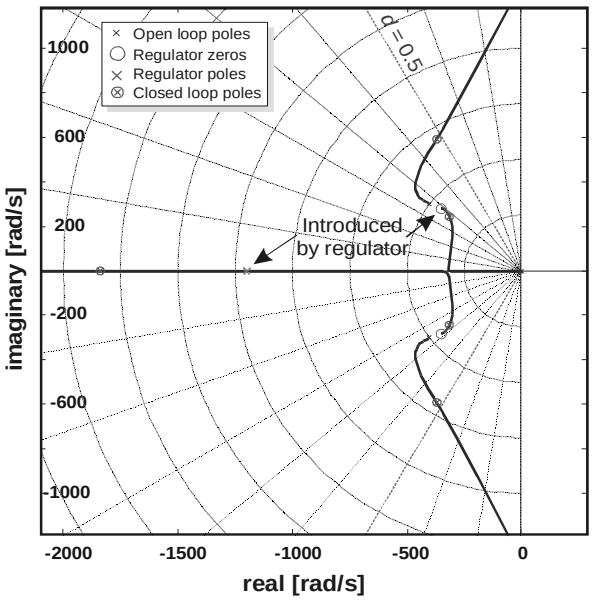

Fig. 16: *Pole zero map of a 2nd order regulator at nominal servo valve parameters and $k_{SPC} = 6$*

The forward gain k_{SPC} can be further increased, when the double real pole of the regulator ($d_{RP} = 1$, ω_{RP} to be maximized) is moved further left. If, for example, the pole frequency ω_{RP} is moved from $\omega_{RP} = 1200$ rad/s (as shown in Fig. 16) to $\omega_{RP} = 2400$ rad/s, a forward gain increase form $k_{SPC} = 6$ to $k_{SPC} = 15$ (!) is achievable at least for *nominal* valve dynamics at identical closed-loop damping of $d_{CP} > 0.5$. This effect can be explained by the fact that for higher regulator pole eigenfrequencies the pole centre of the combined plant (regulator and pump control system dynamics) is dragged further left.

However, the robust design problem – which is here the calculation of the best combination of the regulator zeros d_{RZ} and ω_{RZ} – needs to be solved at the given parameter range of the servo valve. By freezing d_{RP} and ω_{RP} the design is reduced from a five-dimensional to a three-dimensional problem, which can be solved iteratively by increasing the gain k_{SPC} stepwise while optimising the remaining two variables ω_{RZ} and d_{RZ}. The following scheme was carried out for the design process:

1. Define the desired pole region for the closed-loop poles.
2. Maximize ω_{RP} to the maximum allowed frequency of the controller hardware; use $d_{RP} = 1$.
3. Use the result of the proportional control as a start for k_{SPC}.
4. Carry out the parameter space transformation for the desired pole region and optimise the choice of ω_{RZ} and d_{RZ}.
5. Is joint stability achieved for the given forward gain k_{PSC} from step 3? If yes, increase k_{SPC} and repeat step 4 until joint stability region is no longer achieved.

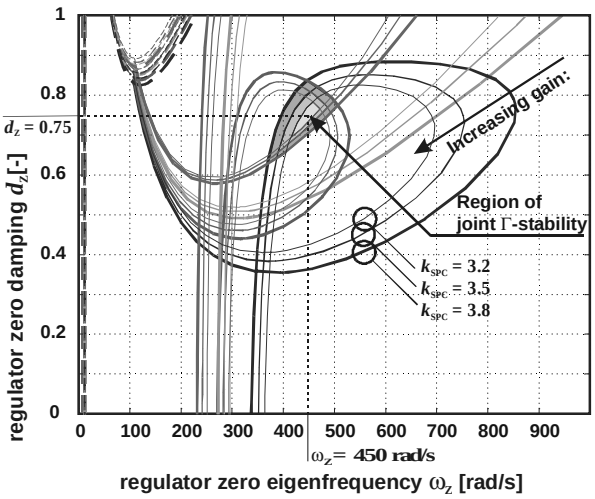

Fig. 17: *Parameter plane of ω_{RZ} and d_{RZ}*

This process will find the maximum gain for the given design problem. Figure 17 shows the parameter plane of ω_{RZ} and d_{RZ}, while increasing the forward gain k_{SPC} at from $k_{SPC} = 2.1$ V_{SV}/V_{LVDT} to $k_{SPC} = 2.8$ V_{SV}/V_{LVDT}. For $k_{SPC} > 3.0$ V_{SV}/V_{LVDT} the joint stability area disappears. The centre of the joint stability region for $k_{SPC} = 2.8$ V_{SV}/V_{LVDT} was chosen as parameters for the zeros for compensation of the servo valve dynamics, giving $\omega_{RZ} = 420$ rad/s and $d_{RZ} = 0.78$. Though, this result shows, that choosing $\omega_{RZ} = \omega_{SV,\,nom}$ and $d_{RZ} = d_{SV,\,nom}$ will not find the optimal solution, neither does one of the corners of any combination of [$\omega_{SV,\,min}$, $\omega_{SV,\,max}$, $d_{SV,\,min}$, $d_{SV,\,max}$].

Table 1: Controller parameters

Parameter Set/Denomination	**Optimised**	**Frozen prior to design**		**Optimised**	
	Gain	Pole freq.	Pole damp.	Zero freq.	Zero damp.
	k_{SPC} [V_{SV}/V_{LVDT}]	ω_{RP} [rad/s]	d_{RP} [-]	ω_{RZ} [rad/s]	d_{RZ} [-]
P14, Proportional	1.4	-	-	-	-
FR228, 2nd order compensation	2.8	1200	1	420	0.78
FR556, 2nd order compensation	5.6	2400	1	420	0.78

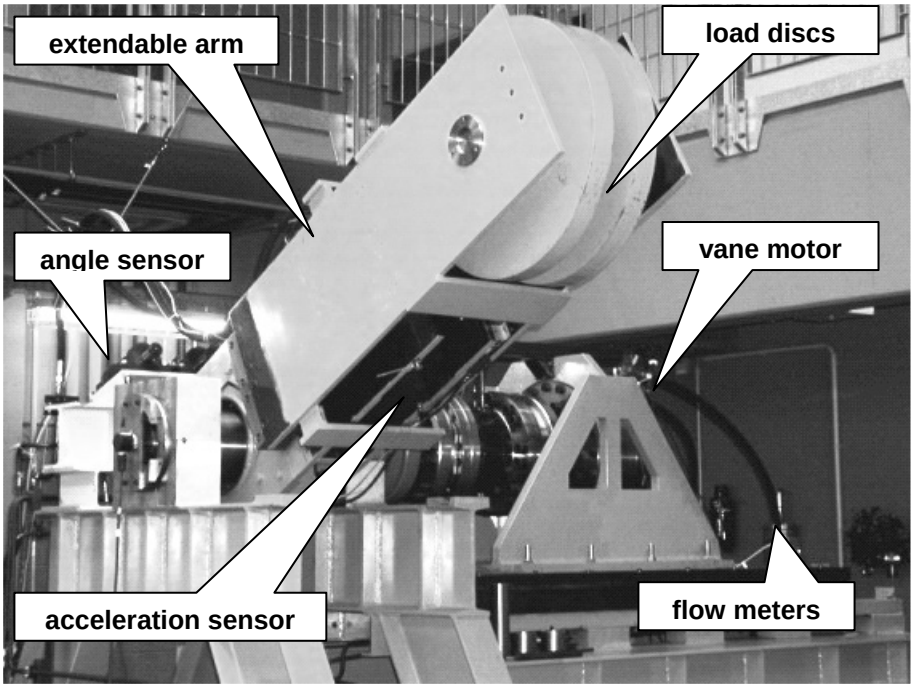

Fig. 18: *Test Rig for Displacement Controlled Rotary Vane Actuator – Demonstrator Load Arm*

As mentioned before, for an increased eigenfrequency of the regulator poles the forward gain can be further increased. For comparison a second controller optimisation was carried out for a doubled regulator pole eigenfrequency of ω_{RP} = 2400 rad/s, where, however, the optimised parameters change slightly. Table 1 shows the final controller parameters for the 2nd order regulator of the swash plate in comparison to proportional control.

7 Experimental Results

For experimental validation the different control schemes were implemented at a test rig, using a sampling time of T = 1 ms and the bilinear transformation rule for time discrete implementation. Figure 18 shows a photograph of the test rig, Fig. 19 illustrates the structure. The pump unit consists of the main axial piston pump (1) and an additional integrated pre-charge pump (2) for supplying the adjustment system and pre-charging the main power lines (port A and port B). It should be noted here that the test rig configuration did not allow the usage of an external reservoir. Therefore, the inlet of the pre-charge pump was fed by an external hydraulic unit (15) via a pressure reduction valve (16). The swash plate is adjusted by a symmetrical adjustment cylinder (3), controlled by a single stage servo valve (4). The position of the adjustment cylinder is measured by an LVDT (5) and fed back to the pump control electronics (6), where an analog proportional controller is installed, giving its control signal to the valve amplifier. This standard controller is disconnected and the (output) position signal of the LVDT and the (input) signal to the valve amplifier are connected to an external controller card (7) installed in a standard PC (8). Here, higher order control laws are implemented and investigated as well as the measured data recorded. The load pressure is adjusted by an adjustable load connected to the vane type hydraulic motor (9). The load pressure is measured using two pressure sensors (10), an additional pressure sensor (11) was used to measure the supply pressure of the adjustment system. The pump shaft is driven by a direct current electrical motor with adjustable speed (13) via a constant transmission gear (14), allowing a second consumer to be connected to the same motor. A further description of the load unit of the test rig can be found in Grabbel and Ivantysynova (2001) and Grabbel (2003). Table 2 lists all relevant parameters that were also used for robust numerical controller design.

Table 2: Test rig parameters

Denomination	Symbol	Value
pump control cylinder diameter	d_{AC}	25.4 mm
pump control cylinder neutral (centred) position	x_H	11.6 mm
pump control cylinder lever arm	r_{AC}	30.0 mm
pump control system supply pressure	p_S	60 bar
servo valve stroke	$y_{SV,\,max}$	0.28 mm
servo valve control voltage	$u_{SV,\,max}$	10 V
servo valve rated flow at 70 bar pressure difference	$Q_{SV@70bar}$	25 l/min

Parameters not relevant for controller design:

Denomination	Symbol	Value
number of pump pistons	z	7
Max. displacement volume of the variable displacement pump	$V_{P,\,nom}$	10.8 cm³/rev
rated shaft speed	n_{nom}	3000 rpm
maximum shaft speed	n_{max}	3600 rpm

Figure 20 shows a comparison of the parameter sets P14, FR214 and FR228 of Table 6.2 (where FR214 uses identical parameters of FR228, but the forward gain identical to P14). The figure shows the swash plate response for step commands of 5%, 10%, 20% and 50% at a load pressure about 100 bar at the pump working pistons. Due to signal noise and pressure related swash plate oscillations (caused by the basic principle of a piston pump) low pass filtering of the swash plate response was necessary to distinguish the signal from the permanent swash plate oscillations. The required time for a 95% rise ($T_{95\%}$ - the time, when 95% of the commanded step is reached) is given in Table 3 for the different parameter sets, considering the effect of the low pass signal filtering.

It can be seen from Table 3 that a 2nd order forward regulator (according to the previously outlined design scheme) basically improves the low level signal response, where a significant reduction of the rise time $T_{95\%}$ is observed. This reduction can already be seen, when proportional control and the forward regulator uses identical forward gain (k_{SPC} = 1.4). Here a reduction of $T_{95\%}$ of almost 50 % for a 5 % step command and of nearly 30 % for a 10 % step command is achieved. When using the maximum forward gain for the 2nd order regulator (k_{SPC} = 2.8) without violating the damping requirement (d_{min} = 0.5) the rise time $T_{95\%}$ for

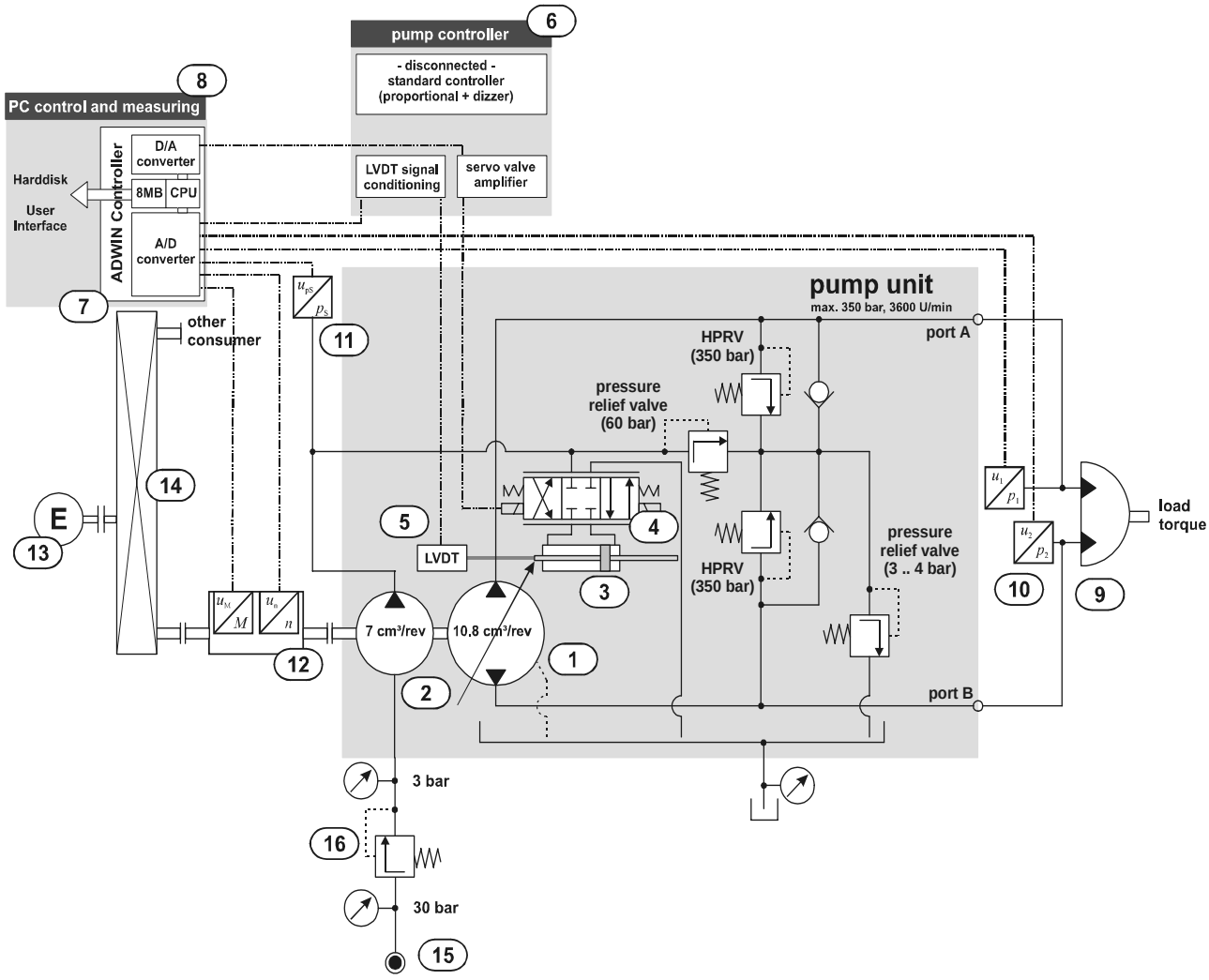

Fig. 19: *Displacement Controlled Rotary Vane Actuator – Test Rig Hydraulic Diagram*

Table 3: Rise time $T_{95\%}$

Commanded step size	**Δx =**	**5 %**	**10 %**	**20 %**	**50 %**
		Rise time $T_{95\%}$ [ms] =			
P14, proportional control, k_{SPC} = 1.4		70	29	22	33
FR214, 2nd order regulation, k_{SPC} = 1.4, ω_{RP} = 1200 rad/s		36	21	22	34
FR228, 2nd order regulation, k_{SPC} = 2.8, ω_{RP} = 1200 rad/s		15	15	17	32
FR256, 2nd order regulation, k_{SPC} = 5.6, ω_{RP} = 2400 rad/s		12	15	19	36

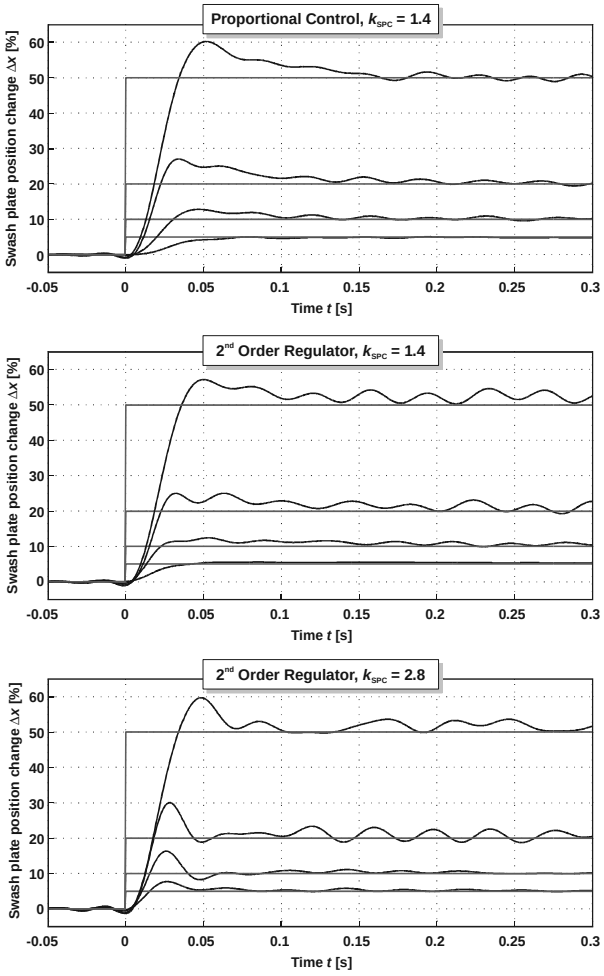

Fig. 20: *Swash plate step response for 5 %, 10 %, 20 % and 50 % command signals.*

a 5 % step is reduced by nearly 80 % (!) and even the rise time for a 20 % step is reduced by 23 %. On the other hand, the rise time for a 50 % step remains more or less constant, what can be explained by the flow saturation of the servo valve. From Table 3 it can also be taken, that the shift of the regulator pole pair to higher frequencies (FR256) does reduce the rise time much further. On the contrary, the rise time for a 20 % step and a 50 % step were measured slightly higher than before, what may also be caused by measurement error and inaccuracy due to filtering and measurement noise.

8 Summary

The paper shows that the commonly found prejudice that pump controlled systems suffer from slow dynamics of the servo pump used as final control element are *not* justified. A non-linear model was developed and it was shown, that in contrast to typically known hydraulic actuator systems, here, not the hydraulic eigenvalues are dominant but the servo valve eigenvalues are. Furthermore, it was shown that a linearization of the dominant part of the system is possible and useful. By using linear control theory, the derived results are easily applicable to existing pump design and available electro-hydraulic control systems. The robustness of the derived controllers was analysed by using the Ackermann parameter space method, taking basically the variable behaviour of the servo valve as the most dominant element into account, since the dominance analysis has shown, that geometric parameters have no effect to control system layout except from flow saturation effects. Furthermore, the results were implemented into an existing test rig and the effect is shown via recording typical step responses.

The results show, that a change of the swash plate controller from proportional control to a second order regulating function achieves a significant reduction of response time of the servo pump swash plate (and thus the delivered flow), especially for low level responses, where the response time is reduced by 50 % and more. This makes this control scheme with its significantly improved adjustment system dynamics very suitable for advanced controller design of the main circuit, controlled by the servo pump, such as acceleration or pressure feedback - see Grabbel and Ivantysynova (2001) for a detailed investigation and experimental results on these control concepts. Also displacement control actuators with superimposed active damping schemes will benefit from improved dynamics of the pump adjustment system.

It has to be noted, that these improvements are possible due to the fact that an overshoot of the swash plate is tolerated (by using d_{min} = 0.5), as long as the swash plate dynamics are significantly higher than the dominant dynamics of the main circuit. For actuators of mobile machinery this constraint is always fulfilled due to the high inertia acting on the actuator and its high oil volume (causing a rather low hydraulic stiffness).

The controller design scheme for a second order swash plate regulator is rather simple as long as frequency and damping intervals of the servo valve, controlling the swash plate adjustment cylinder position,

are known. A spread of the servo valve frequency of 50 % (ω_{SV} = 400 .. 600 rad/s) and of approx. 40 % in damping (d_{SV} = 0.7 .. 1.0) were considered – typical values for standard servo valves. Since typical pump control systems use rather small cylinders, the hydraulic stiffness of the system is rather high and the hydraulic properties and the geometry of the system do not influence the achievable dynamics of *an appropriate controller design*. This does, however, *not mean*, that basic design parameter does not influence the response time! Especially for rather high swash plate step commands (20 % and more), the servo valve flow saturation and consequently the geometry of the pump control cylinder limit the achievable rise time. In order to improve the dynamics at higher step commands it is necessary to reduce size and stroke of the pump control cylinder as much as possible, which requires precise knowledge of the forces, acting on the pump control cylinder. A design optimisation should reduce the piston diameter A_{AC} and the effective lever arm l_{AC} of the pump control (in order to reduce the required stroke) as much as possible. This consequently leads to higher control pressures and a higher supply pressure of the control system.

The paper has demonstrated that with advanced control concepts swash plate control systems of high dynamics can be realized. The concepts have been proven experimentally. In the meantime they have been already used for realization of displacement controlled rotary and linear actuators. Both advanced actuator solution (linear and rotary) have been tested in the laboratory of the authors, see Grabbel (2003) and Rahmfeld (2002). The linear actuator using a single rod cylinder was already tested in a mobile machine in field tests, see Rahmfeld et.al (2004).

Nomenclature

β	swash plate angle	[°]
ω_{AC}	effective adjustment system eigenfrequency	[rad/s]
Θ_{AS}	effective inertia of the adjustement system with respect to its rotational axis	[kgm²]
ω_{CP}	eigenfrequency of the closed loop dominant pole pair	[rad/s]
ω_{RP}	regulator pole eigenfrequency	[rad/s]
ω_{ZP}	regulator zero eigenfrequency	[rad/s]
ω_{SV}	eigenfrequency of the servo valve	[rad/s]
φ_i	angular position of current working piston	[°]
$\varphi_{command}$	commanded axis angle	[°]
φ_{axis}	actual axis angle	[°]
Δp	differential pressure	[Pa]
Δp_{AC}	differential pressure at the adjustment cylinder	[Pa]
Δp_{OP}	differential pressure at operating (= linearization) point	[Pa]
ω_{RP}	regulator pole eigenfrequency	[rad/s]
ω_{RZ}	regulator zero eigenfrequency	[rad/s]
A_{AC}	piston area	[m²]
c	spring coefficient	[N/m]
B	servo valve constant	$[(m^5/kg)^{1/2}]$
C_H	hydraulic capacitance	[m/N]
$C_{H,A}$	hydraulic capacitance of chamber A	[m/N]
$C_{H,B}$	hydraulic capacitance of chamber B	[m/N]
C_p	pressure amplification	[m³/s/Pa]
C_y	volume flow amplification	[m²/s]
d_{AC}	effective system damping	[-]
d_{CP}	damping of the closed loop dominant pole pair	[-]
d_{RP}	regulator pole damping	[-]
d_{RZ}	regulator zero damping	[-]
d_{SV}	servo valve damping	[-]
f_C	coefficient of Coulomb friction	[N]
f_s	coefficient of static friction	[N]
f_{SV}	servo valve frequency	[Hz]
f_v	coefficient of viscous friction	[Ns/m]
$F_{\Delta p}$	pressure force of pump control cylinder	[N]
F_F	friction force	[N]
F_S	spring force	[N]
F_{SL}	self adjusting forces acting on pump control cylinder	[N]
i	counting index	[-]
i_{SV}	servo valve input signal (current)	[A]
k_i	controller prameters	[-]
k_{LA}	coefficient of external leakage of chamber A	[m³/s/Pa]
k_{LB}	coefficient of external leakage of chamber B	[m³/s/Pa]
k_{Li}	coefficient of internal leakage	[m³/s/Pa]
k_{SPC}	forward gain swash plate control	[-]
k_{SV}	servo valve amplification	[m/V]
K_{Oil}	oil bulk modulus	[N/m²]
m_{equ}	effective mass of the swash plate system with respect to the adjustment cylinder	[kg]
M_{Sx}	swash plate moment about x-axis	[m]
p_A	cylinder pressure in chamber A	[Pa]
p_B	cylinder pressure in chamber B	[Pa]
p_e	pump case pressure	[Pa]
p_i	Instantaneous cylinder pressure of each piston	[Pa]
p_R	return line pressure	[Pa]
p_S	pump control system supply pressure	[Pa]
Q_A	volume flow to chamber A	[m³/s]
Q_B	volume flow to chamber B	[m³/s]
Q_L	leakage flow	[m³/s]
r	cylinder lever arm	[m]
R	piston pitch radius	[m]
u_{SV}	servo valve control voltage	[V]

u_x	output signal of pump control cylinder position sensor	[V]
u_{SV}	servo valve input voltage	[V]
V_A	volume of cylinder chamber A	[m³]
V_B	volume of cylinder chamber B	[m³]
V_{dead}	dead volume of cylinder, including lines	[m³]
x	piston position of pump adjustment cylinder	[m]
x_H	neutral (centred) position of the adjustment cylinder	[m]
y	spool position of the pump control valve	[m]
y_{OP}	spool position at operating (= linearization) point	[m]

A	system matrix
B	input matrix
C	output matrix
D	feedthrough matrix with index $_{AS}$ for adjustment system
x	state vector of state space model
x_1 .. x_3	individual elements of the state vector

$G(s)$	transfer function
$K(s)$	controller transfer function
$p_{1,2}$	poles

References

Ackermann, J. et al. 2000. *Robust Control – Systems with Uncertain Physical Parameters*. Springer, London, UK.

Backé, W. 1993. Recent research projects in hydraulics. *Proceedings of second JHPS International Symposium on Fluid Power*. Tokyo, Japan.

Bahr Khalil, M.K., Yurkevich, V., Svoboda, J., Bhat, R.B. 2002. Implementation of Single Feedback Control Loop For Constant Power Regulated Swash Plate Axial Piston Pumps. *International Journal of Fluid Power*, Vol.3, No.3.

Berbuer, J. 1988. *Neuartige Servoantriebe mit primärer Verdrängersteuerung*. Dissertation, RWTH Aachen, Germany.

Berg, H. and Ivantysynova, M. 1999. Design and testing of a robust linear controller for secondary controlled hydraulic drive. *Journal of Systems and Control Enginering. Proceedings of the Institution of Mechanical Engineers* Vol. 213 Part I, pp.375-386.

Berg, H. 1999. *Robuste Regelung verstellbarer Hydromotoren am Konstantdrucknetz*, Dissertation, Gerhard-Mercator-Universität Duisburg, Germany. Fortschritt-Berichte VDI, Reihe 8, No. 764, VDI Verlag, Düsseldorf, Germany.

Grabbel, J. and Ivantysynova M. 2001. Control strategies for Joint Integrated Servo Actuators in mobile machinery. *7th Scandinavian International Conference on Fluid Power*, Linköping, Sweden.

Grabbel, J. 2003. *Robust Control Strategies for Displacement Controlled Rotary Actuators using Vane Type Motors.* Dissertation, Technical University of Hamburg-Harburg, Germany. Fortschritt-Berichte VDI, Reihe 8, No. 1029, VDI Verlag, Düsseldorf, Germany.

Haas, H.-J. 1989. *Sekundärgeregelte hydrostatische Antriebe im Drehzahl- und Drehwinkelregelkreis.* Dissertation, RWTH Aachen, Germany.

Hahmann, W. 1973. *Das dynamische Verhalten hydrostatischer Antriebe mit Servopumpe und ihr Einsatz in Regelkreisen.* Dissertation, RWTH Aachen, Germany.

Ivantysyn, J. and Ivantysynova M. 2000. *Hydrostatic Pumps and Motors - Principles, Designs, Performance, Modelling, Analysis, Controll and Testing.* Academica Books International, New Delhi.

Ivantysynova, M. et al. 2002. Prediction of Swash Plate Moment Using the Simulation Tool CASPAR. *International Mechanical Engineering 2000 Congress and Exposition, IMECE2002-39322*, New Orleans, Louisiana, USA.

Metzner, F.T. 1985. *Kennwerte der Dynamik sekundärgeregelter Axialkolbeneinheiten*. Dissertation, Universität der Bundeswehr Hamburg, Germany.

Rahmfeld, R. 2002. *Development and Control of Energy Saving Hydraulic Servo Drives for Mobile Systems.* Dissertation, Technical University of Hamburg-Harburg, Germany. Fortschritt-Berichte VDI, Reihe 12 No. 527, VDI Verlag, Düsseldorf, Germany.

Rahmfeld, R. et al. 2004. Displacement Controlled Wheel Loader – a simple and clever Solution. *Proc. of the 4th International Fluid Power Conference (4. IFK)*, Dresden, Germany, Vol. 2, pp. 183 - 196.

Roth, J. 1983. *Regelungskonzepte für lagegeregelte, elektrohydraulische Servoantriebe.* Dissertation, RWTH Aachen, Germany.

Sprockhoff, V. 1979. *Untersuchungen von Regelungen am hydrostatischen Zylinderantrieb mit Servopumpe*. Dissertation, RWTH Aachen, Germany.

Wieczorek, U. and Ivantysynova, M. 2002. Computer Aided Optimization of Bearing and Sealing Gaps in Hydrostatic Machines - the Simulation Tool CASPAR. *International Journal of Fluid Power 3 (2002) No. 1, pp. 7-20*.

Ziegler, R. 1990. *Auslegung und Optimierung schneller Servopumpen*. Dissertation, Universität Karlsruhe, Germany.

Joerg Grabbel
Born on February 5th 1970 in Hamburg (Germany). Study of Mechanical Engineering at the Technical University of Hamburg-Harburg (TUHH). Diploma Thesis in 1997 at the Institute for Aircraft Systems Engineering From 1997 to 1999 Scientific Employee at the Department of Measurement and Control Engineering of the Gerhard Mercator University of Duisburg. From 1999 to 2002 Scientific Employee at the Institute for Aircraft Systems Engineering at the TUHH, where he received his PhD in 2003. Since 2003 he is employed at B+V Industrietechnik GmbH (formerly Blohm+Voss), where he is responsible for electro-hydraulic fin stabilizer and steering gear control.

Monika Ivantysynova
Born on December 11th 1955 in Polenz (Germany). She received her MSc. Degree in Mechanical Engineering and her PhD. Degree in Fluid Power from the Slovak Technical University of Bratislava, Czechoslovakia. After 7 years in fluid power industry she returned to university. In April 1996 she received a Professorship in fluid power & control at the University of Duisburg (Germany). From 1999 until August 2004 she was Professor of Mechatronic Systems at the Technical University of Hamburg-Harburg. Since August 2004 she is Professor at Purdue University, USA. Her main research areas are energy saving actuator technology and model based optimisation of displacement machines as well as modelling, simulation and testing of fluid power systems. Besides the book “Hydrostatic Pumps and Motors” published in German and English, she has published more than 80 papers in technical journals and at international conferences